

# TG-43 U1 based dosimetric characterization of model 67-6520 Cs-137 brachytherapy source

Ali S. Meigooni<sup>a)</sup>

Department of Radiation Medicine, North Shore University Hospital, 300 Community Drive, Manhasset, New York 11030 and Department of Radiation Medicine, University of Kentucky Chandler Medical Center, Lexington, Kentucky 40536-0084

Clarissa Wright, Rafiq A. Koon, and Shahid B. Awan

Department of Radiation Medicine, University of Kentucky Chandler Medical Center, Lexington, Kentucky 40536-0084

Domingo Granero

Department of Radiation Physics, ERESA, Hospital General Universitario, Avenida Tres Cruces, 2, E-46014 Valencia, Spain

Jose Perez-Calatayud

Department of Oncology, Physics Section, "La Fe" University Hospital, Avenida Campanar 21, E-46009 Valencia, Spain

Facundo Ballester

Department of Atomic, Molecular and Nuclear Physics, University of Valencia, C/ Dr. Moliner 50, E-46100 Burjassot, Spain and Instituto de Física Corpuscular (IFIC), C/ Dr. Moliner 50, E-46100 Burjassot, Spain

(Received 15 March 2009; revised 19 August 2009; accepted for publication 19 August 2009; published 16 September 2009)

**Purpose:** Brachytherapy treatment has been a cornerstone for management of various cancer sites, particularly for the treatment of gynecological malignancies. In low dose rate brachytherapy treatments,  $^{137}\text{Cs}$  sources have been used for several decades. A new  $^{137}\text{Cs}$  source design has been introduced (model 67-6520, source B3-561) by Isotope Products Laboratories (IPL) for clinical application. The goal of the present work is to implement the TG-43 U1 protocol in the characterization of the aforementioned  $^{137}\text{Cs}$  source.

**Methods:** The dosimetric characteristics of the IPL  $^{137}\text{Cs}$  source are measured using LiF thermoluminescent dosimeters in a Solid Water<sup>TM</sup> phantom material and calculated using Monte Carlo simulations with the GEANT4 code in Solid Water<sup>TM</sup> and liquid water. The dose rate constant, radial dose function, and two-dimensional anisotropy function of this source model were obtained following the TG-43 U1 recommendations. In addition, the primary and scatter dose separation (PSS) formalism that could be used in convolution/superposition methods to calculate dose distributions around brachytherapy sources in heterogeneous media was studied.

**Results:** The measured and calculated dose rate constants of the IPL  $^{137}\text{Cs}$  source in Solid Water<sup>TM</sup> were found to be  $0.930(\pm 7.3\%)$  and  $0.928(\pm 2.6\%) \text{ cGy h}^{-1} \text{ U}^{-1}$ , respectively. The agreement between these two methods was within our experimental uncertainties. The Monte Carlo calculated value in liquid water of the dose rate constant was  $\Lambda = 0.948(\pm 2.6\%) \text{ cGy h}^{-1} \text{ U}^{-1}$ . Similarly, the agreement between measured and calculated radial dose functions and the anisotropy functions was found to be within  $\pm 5\%$ . In addition, the tabulated data that are required to characterize the source using the PSS formalism were derived.

**Conclusions:** In this article the complete dosimetry of the newly designed  $^{137}\text{Cs}$  IPL source following the AAPM TG-43 U1 dosimetric protocol and the PSS formalism is provided. © 2009 American Association of Physicists in Medicine. [DOI: [10.1118/1.3224462](https://doi.org/10.1118/1.3224462)]

Key words: brachytherapy, Cs-137, PSS model, dosimetry, GEANT4, TG-43

## I. INTRODUCTION

Soon after the discovery of  $^{226}\text{Ra}$ , the importance of the clinical application of brachytherapy sources was discovered.<sup>1</sup> However, problems of using  $^{226}\text{Ra}$  sources due to the production of radon gas and the possibility of breakdown of the source capsule and its releasing into the patients were some of the strong motivators to find and use alternative radioactive materials.<sup>2</sup>  $^{137}\text{Cs}$  sources were introduced as

a substitute for  $^{226}\text{Ra}$  in brachytherapy implants and have been used for several decades for low dose rate (LDR),<sup>3</sup> most commonly in treatment of gynecological cancer patients, through intracavitary implants.<sup>4</sup>

A historical review of the existing publications will give an idea regarding the current status of dosimetric characterization for  $^{137}\text{Cs}$  sources. In 1968, Meisberger *et al.*<sup>5</sup> measured the effective attenuation of different gamma-emitter

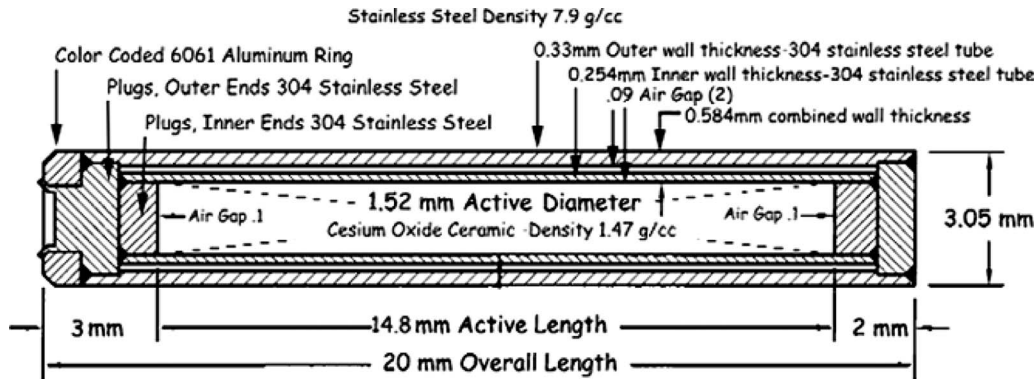


FIG. 1. Schematic diagram of the model 67-6520  $^{137}\text{Cs}$  source (courtesy of the Isotope Product Laboratories). The source tip is at the side of the aluminum ring.

radionuclides, including  $^{137}\text{Cs}$ , in water as compared to air. However, they did not determine the source self-absorption and anisotropy of the radiation distribution around the sources. In 1972, Krishnaswamy<sup>6</sup> showed the effects of oblique filtration through walls in  $^{137}\text{Cs}$  needles and tubes as compared to equivalent radium sources. Based on this information, he calculated the dose distribution around  $^{137}\text{Cs}$  sources, with different active lengths, using an along-and-away format (limited up to 5 cm distance from the source center). Despite the differences in the geometric structures of various source models, the Krishnaswamy data are still being used for a quick hand calculation or double check in brachytherapy procedures with LDR  $^{137}\text{Cs}$  sources. In 1988, Williamson<sup>7</sup> presented dose rate tables and treatment planning data for two newly designed  $^{137}\text{Cs}$  sources, namely, gold matrix (series 67-800, intracavitary source, by Radiation Therapy Resources, Inc., Valencia, CA) and a discrete seed source (Oris Intracavitary tube source from CIS-US, Inc., Lake Success, NY). The Monte Carlo generated dose rate tables are presented in an along-and-away format, which are utilized in the Sievert integral based treatment planning systems. In 1989, Waggener *et al.*<sup>8</sup> wrote a computer program to generate the dose distribution around an asymmetric  $^{137}\text{Cs}$  source (3M). They confirmed the accuracy of the calculated dose rate values by comparison with measured data using the Fricke dosimeter. The angular distributions of the dose rates for different radial distances are presented in a tabulated format. They have shown that the asymmetric distribution of the  $^{137}\text{Cs}$  leads to a large difference (67%) between the dose rates at the two ends of the source (radial distance of 1 cm). These differences decrease to less than 10% at points lying more than 3 cm from the source center. Using Monte Carlo simulation, in 1998, Williamson<sup>9</sup> calculated dose rate distributions around the Amersham CDCS.J type  $^{137}\text{Cs}$  source and also updated the dosimetric information of the 3M model 6500/6D6C  $^{137}\text{Cs}$  sources. The results and corresponding parameters were utilized in the Sievert integral based treatment planning systems. The above noted investigations were published prior to the original<sup>10</sup> or updated<sup>11</sup> Task Group No. 43 recommendations (TG-43 or TG-43 U1, respectively) by the American Association of Physicist in Medicine (AAPM).

Using the Monte Carlo simulation technique, Casal *et al.*<sup>12</sup> obtained the absolute dose rates around the CDCS-M-type  $^{137}\text{Cs}$  source. These results were presented in both TG-43 parameters and the along-and-away tabulated format. They compared their tabulated results with Krishnaswamy's data<sup>6</sup> for  $^{137}\text{Cs}$  sources and demonstrated that for distances greater than 1 cm the differences were approximately 2% lower, and that these differences rise up to 4% at 0.5 cm. Other published data regarding the TG-43 or TG-43 U1 based dosimetric parametrizations of different  $^{137}\text{Cs}$  source pertains to models CSM11,<sup>13</sup> CSM3-a,<sup>14</sup> CSM2,<sup>17</sup> and CSM3,<sup>15</sup> Walstam CDC.K type,<sup>16</sup> CDC-type miniature,<sup>17</sup> and the Selectron pellet.<sup>18</sup> Liu *et al.*<sup>19</sup> determined the dosimetric parameters of the CSM-type  $^{137}\text{Cs}$  sources based on the original TG-43 formalism. Pérez-Calatayud *et al.*<sup>20</sup> also obtained the two-dimensional (2D) dose rate distribution around the CSM-type  $^{137}\text{Cs}$  sources and compared their results with the calculated parameters by Liu *et al.*<sup>19</sup>

As the production of several of the above noted sources have been discontinued, a new  $^{137}\text{Cs}$  source design has been introduced (model 67-6520, source B3-561) by Isotope Products Laboratories (IPL) to meet the demand of the current clinical procedures. To date, there is no publication on the dosimetric parametrizations of this new source model.

The goal of this work is to determine the dosimetric characteristics of the new  $^{137}\text{Cs}$  source (model 67-6520, source B3-561) using the TG-43 U1 protocol.<sup>11</sup> These determinations will be performed using experimental and Monte Carlo simulation techniques. In addition, the primary and scatter photon dose contributions of the new source will be determined for their application in convolution/superposition dose calculation methods around brachytherapy implant in heterogeneous media.

## II. MATERIALS AND METHODS

### II.A. Source characteristics

Figure 1 shows the schematic diagram of the model 67-6520  $^{137}\text{Cs}$  source manufactured by IPL (24937 Avenue Tibbitts, Valencia, CA) and distributed by Radiation Products Design, Inc. (5218 Barthel Industrial Drive, Albertville, MN). In the following sections we refer to this source as the

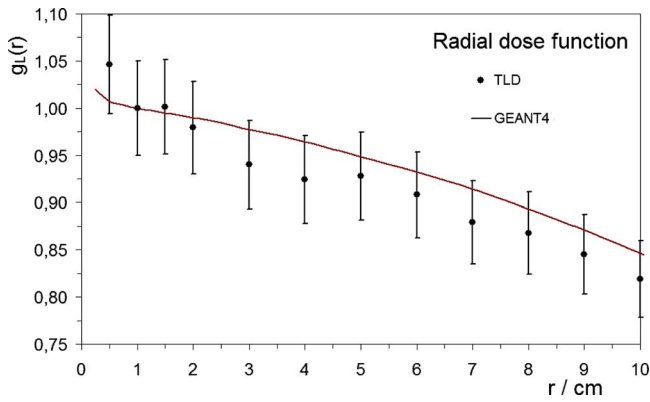


FIG. 2. Comparison between the Monte Carlo simulated (solid line) and measured (symbol) radial dose functions of the IPL  $^{137}\text{Cs}$  source in Solid Water<sup>TM</sup>.

IPL  $^{137}\text{Cs}$  source. The physical dimensions of the IPL  $^{137}\text{Cs}$  source are 3.05 mm in diameter and 20 mm in length. The capsule is composed of two types of 304 stainless steel layers with a total wall thickness of 0.584 mm (outer layer of 0.33 mm, inner layer of 0.254 mm). The active portion of the source is 1.52 mm in diameter and 14.8 mm in length. The radioisotope is uniformly distributed in the core of the ce-

sium oxide ceramic source, assuming approximately 5.29 mg  $\text{Cs}_2\text{O}$  in a 50 mCi source. The density of the active ceramic material is  $1.47 \text{ g/cm}^3$  while the density of the ceramic itself is  $1.27 \text{ g/cm}^3$ . A color coded aluminum ring easily identifies the source activity and defines the source tip. The active core is placed nonsymmetrically within the capsule with its tip and end located at 3 and 2 mm, respectively, from the capsule. The calibration of the air-kerma strength of this source is traceable to the primary standards by the National Institute of Standard and Technology (NIST) through the Accredited Dosimetric Calibration Laboratory (ADCL) at the University of Wisconsin, Madison. The source calibration has been performed by the vendor (Eckert & Ziegler Isotope Products, Valencia, CA) prior to its shipment to our institution for dosimetric evaluation. A secondary calibration system has been developed at our institution using a Capintec CRC-7R well-type chamber for daily verification process.

**II.B. Experimental setup characteristics for thermoluminescent dosimeter measurements in Solid Water<sup>TM</sup>**

Dosimetric characteristics of the IPL  $^{137}\text{Cs}$  source were determined experimentally using  $1.0 \times 1.0 \times 1.0$  and  $3.1 \times 3.1 \times 0.89 \text{ mm}^3$  TLD-100 LiF thermoluminescent dosim-

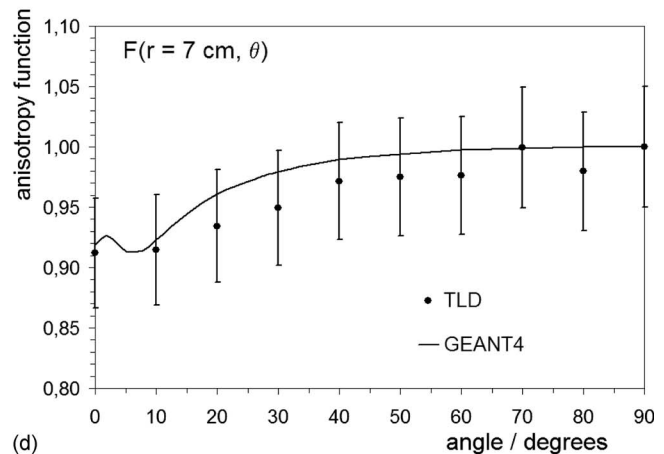
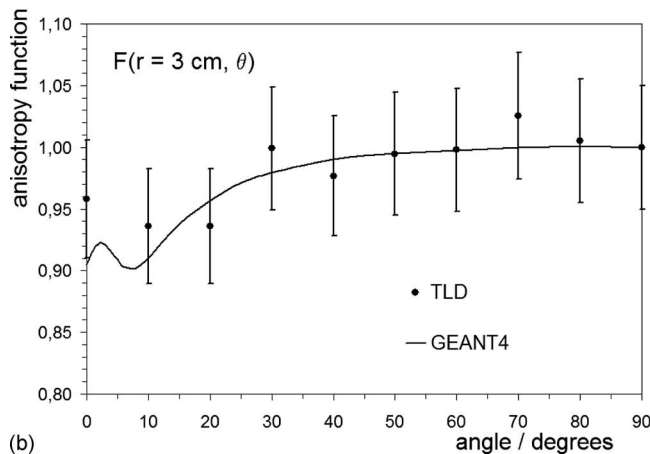
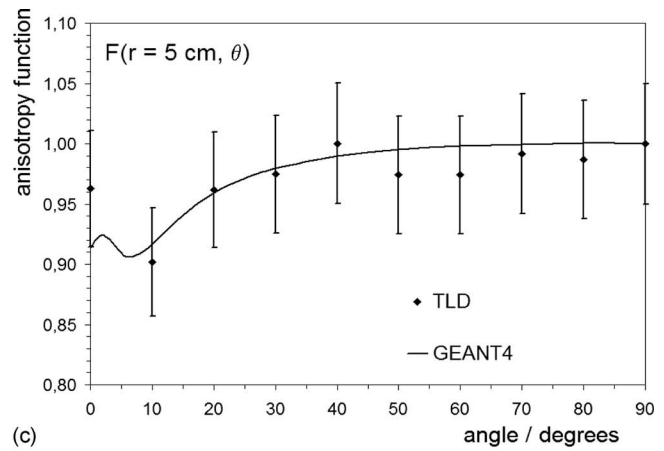
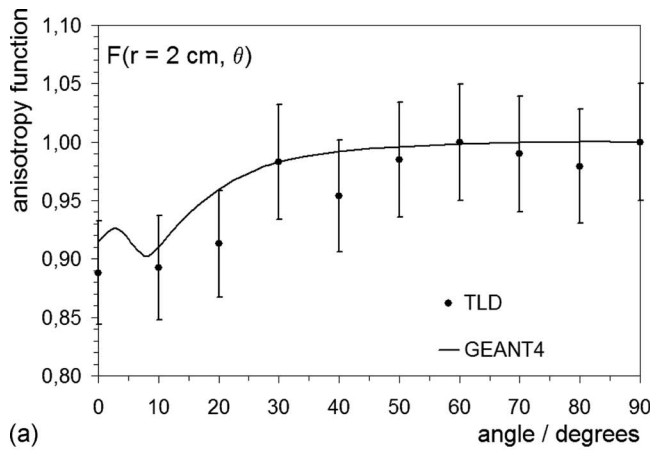


FIG. 3. Monte Carlo calculated radial dose functions for the IPL source. These data was fitted to a 5<sup>th</sup> order polynomial with coefficients  $a_0=1.00765$ ,  $a_1=-7.073 \times 10^{-3} \text{ cm}^{-1}$ ,  $a_2=-5.680 \times 10^{-4} \text{ cm}^{-2}$ ,  $a_3=-1.376 \times 10^{-5} \text{ cm}^{-3}$ ,  $a_4=1.117 \times 10^{-6} \text{ cm}^{-4}$ , and  $a_5=-1.608 \times 10^{-8} \text{ cm}^{-6}$  between 0.25 and 20 cm.

eters (TLDs) (TLD-100, Harshaw/Bicron 6801 Cochran Rd., Solon, OH 44139) in a  $30 \times 30 \times 25$  cm<sup>3</sup> Solid Water™ phantom. Our TLD procedures have been described in detail in our previous publications.<sup>21,22</sup> As described in these publications, slabs of the Solid Water™ phantom (Radiation Measurements Inc., RMI, Middletown, WI) were custom designed and machined to accommodate the brachytherapy source and TLD chips for a particular dosimetric procedure.

One of these slabs of Solid Water™ was designed for measurement of the radial dose function and dose rate constant. Four TLD chips, separated by 90° from each other, were placed at each radial distance, on the transverse bisector plane of the source. In addition, the positions of the TLDs within the phantom were selected in a specific pattern in order to minimize interference of any one TLD to the absorbed dose of any other TLD chip. A cylindrical plug was designed to hold the source in the desired position and also facilitate a rapid placement and removal of the source within the phantom setup. The radial dose function was measured at radial distances ranging from 0.5 to 10 cm, with 0.5 cm increments from 0.5 to 2 cm, and with 1 cm increments from 2 to 10 cm. Dose rate constant was obtained from the TLDs located at 1 cm radial distance from the source. The final dose rate constant was extracted from the average of at least 20 TLD chips.

Another Solid Water™ phantom material slab was designed for measurement of 2D anisotropy function of the IPL <sup>137</sup>Cs model<sup>21,22</sup> according to the TG-43 U1 protocol.<sup>11</sup> In this slab, the TLDs were arranged in a circular fashion at radial distances of 2, 3, 5, and 7 cm from the source center. Measurements were performed in angular increments of 10° from 0° to 350°. With this design, either two sets of data points from 0° to 180° or four sets of data points in the range of 0°–90° have been obtained.

The irradiated TLDs were read using a Harshaw model 3500 TLD reader and was annealed using a standard annealing technique.<sup>23</sup> The response or readout (also known as TL) of the TLD chips was converted to dose by calibrating the responses of several TLD chips from the same set using the 6 MV photons beams from a Varian 2100CD linear accelerator. The TLD calibrations were performed using Solid Water™ phantom material ( $20 \times 20 \times 20$  cm<sup>3</sup>). One of the slabs of the phantom materials was accurately machined to accommodate the TLD chips in a plane perpendicular to the central axis of the beam. The TLD chips were placed at the depth of the maximum dose, around the central axis of the beam, with the calibration beam geometry (i.e., 100 cm SSD and  $10 \times 10$  cm<sup>2</sup> field size). Five TLD chips were exposed to 25 cGy and five were exposed to 100 cGy. The slope of the linear curve obtained from the readout of these chips to the irradiated dose was found to be the calibration factor of those chips. The output of this linear accelerator had recently been calibrated (monthly QA procedures) with an ion chamber in a water phantom, following the AAPM TG-51 recommendations. The measurements of the dose distributions around the <sup>137</sup>Cs source were carried out by predetermination of the exposure time for a dose range of 10–100 cGy, where the

TLD response is linear.<sup>23</sup> If larger doses are used during the measurements, the calibration dose range increases to cover the maximum dose and also provide the nonlinearity of the TLD response.

## II.C. Monte Carlo calculations

The Monte Carlo transport Code GEANT4 version 8.0<sup>24</sup> was used to calculate the air-kerma and the dose rate distributions around an IPL <sup>137</sup>Cs source in liquid water and in Solid Water™ phantom materials. GEANT4 has been used in dosimetric evaluation of different models of brachytherapy sources, including <sup>137</sup>Cs sources,<sup>20,18</sup> and based on the recommendations in the AAPM-ESTRO prerequisite report, it has been proven to be a well established code in this field.<sup>25</sup>

In the present study, the  $\beta$  spectrum of the <sup>137</sup>Cs source was not considered in the simulations, because its contribution to the dose rate distribution was found to be negligible.<sup>26</sup> Photon interaction models for the Compton scattering, photoelectric effect, and Rayleigh scattering processes were taken from the low energy package of GEANT4. In addition, this code uses the cross section data from the EPDL97 library,<sup>27</sup> as it is recommended in the TG-43 U1 report.<sup>11</sup> In these simulations, the cutoff photon energy was set to be 10 keV.

The track length estimator<sup>28</sup> was used to estimate collision kerma. In this model, it has been assumed that the secondary electrons are under electronic equilibrium condition and the collision kerma is equal to the absorbed dose. Consequently, no electron transport was considered in these simulations. For typical <sup>137</sup>Cs sources, electronic equilibrium is reached at a radial distance of 0.35 cm from the source center.<sup>26</sup> At 0.25 cm kerma is approximately 3% lower than dose.

In order to validate the accuracy of the source design, dimensions, and composition materials used in the Monte Carlo studies, the Monte Carlo simulations were performed in a  $30 \times 30 \times 25$  cm<sup>3</sup> Solid Water™ phantom, which is identical to that used in the experimental setup for TLD measurements. The chemical composition and density of Solid Water™ phantom were described in previous publications.<sup>29</sup> The kerma (to liquid water in Solid Water™) was scored in cylindrical shell tally cells (height and width of 0.05 cm) with their longitudinal axes coincident with the longitudinal axis of the source.

After validation of the Monte Carlo algorithm and accuracy of the source characteristics used in the simulation, dose rate distribution in liquid water was calculated using the same source input data. In these MC simulations, the IPL <sup>137</sup>Cs source was placed at the center of a 40 cm radius spherical liquid water phantom, which was recommended as an unbounded phantom for dose calculation at distances of up to 20 cm from the source center.<sup>30,31</sup> To obtain the dose rate distribution in an along-and-away format,  $\dot{D}(y,z)$ , the kerma rates were scored in  $400 \times 800$  cylindrical shell tally cells (height and width of 0.05 cm) with their longitudinal axes coincident to the longitudinal axis of the source. The second grid system was used to obtain the dose rate distri-

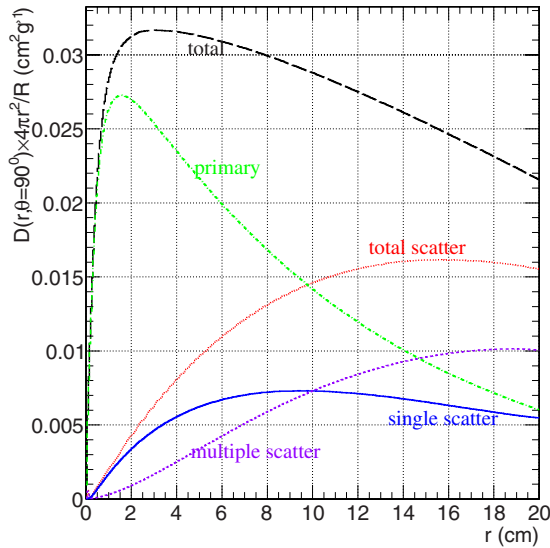


FIG. 4. Separation of the different contributions to dose along the transverse axis of the IPL source. Dose has been normalized to the total emitted radiant energy of photons per unit solid angle,  $R/4\pi$ , and multiplied by the distance to the source squared.

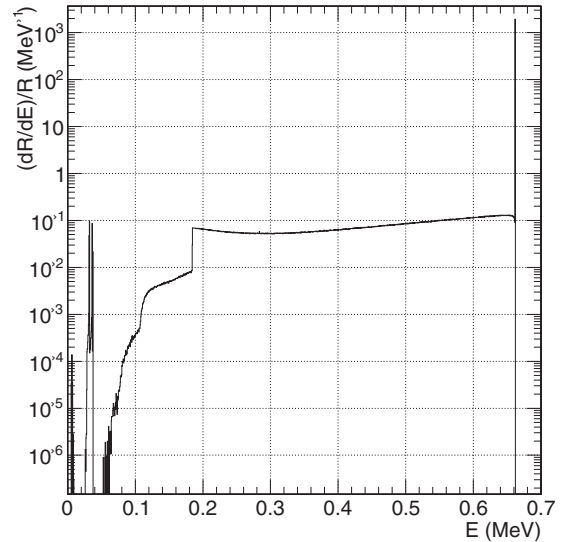


FIG. 5. Energy-weighted photon spectrum per unit emitted radiant energy of photons exiting the IPL source.

butions in polar coordinates,  $\dot{D}(r, \theta)$ , to derive the TG-43 U1 formalism parameters.<sup>11</sup> This grid was composed of  $400 \times 180$  cells bounded by two concentric spheres, 0.05 cm radial differences, and two concentric cones with their apex at the source center,  $1^\circ$  angular width. The center of this tally cell is located at  $(r, \theta)$ .

The air-kerma strength of the IPL  $^{137}\text{Cs}$  source has been determined in the void space according to the TG-43 U1<sup>11</sup> recommendations. The air kerma  $S_K$  was calculated at a distance of 100 cm along the transverse bisector of the source. In these simulations, the tally cell was chosen to be a squared annulus (1 cm thick and 1 cm high) with longitudinal axis coincident with the longitudinal axis of the source.

**II.D. TG-43 U1 dosimetry protocol**

As described in this protocol, the general 2D dose rate equation is defined as

$$\dot{D}(r, \theta) = S_K \Lambda \frac{G_X(r, \theta)}{G_X(1 \text{ cm}, \pi/2)} g_X(r) F(r, \theta), \tag{1}$$

where  $\dot{D}(r, \theta)$  is the dose rate at the point of interest at some distance  $r$  from the center of the source and polar angle  $\theta$  relative to the longitudinal axis of the source,  $S_K$  is the air-kerma strength,  $\Lambda$  is the dose rate constant in water,  $G_X(r, \theta)$  is the geometry function at the point of interest,  $G_X(1 \text{ cm}, \pi/2)$  is the geometry function at the reference point 1 cm from the source and at  $90^\circ$  from the longitudinal axis of the source,  $g_X(r)$  is the radial dose function, and

TABLE I. Propagation of errors estimated for the experimental and Monte Carlo procedures used in the present investigations. The coverage index of the uncertainties is  $k=1$ . The components identified with a “\*” were not utilized for derivation of the total uncertainty in the experimental radial dose function and 2D anisotropy function data, as the data are formed from ratios of measured doses, and are therefore unaffected by the identified components. The underlined italic-bold entries are those that have been used for error bars of the radial dose and anisotropy functions.

Component	TLD measurement uncertainties (%)		Monte Carlo uncertainties (%)	
	Type A	Type B	Type A	Type B
Repetitive measurements	4			
TLD dose calibration (including LINAC calibration)		2.0		
LiF energy correction		5.0*		
Source and TLD position		2.0		
Air-kerma strength		3.0*	0.5	
Statistical uncertainties			0.5	
Cross sections				2.5
Quadrature sum	4	<u>6.5/2.8</u>	0.7	2.5
Total uncertainty		<u>7.3/4.9</u>		<b>2.6</b>

TABLE II. Dose rate per unit air-kerma strength ( $\text{cGy h}^{-1} \text{U}^{-1}$ ) around the IPL source. The  $z$  axis is defined along the source positive toward the source tip. The origin is at the geometric center of the source (not at the active center).

Distance along $z$ (cm)	Distance away $y$ (cm)														
	0	0.25	0.5	0.75	1	1.5	2	2.5	3	4	5	6	8	10	14
-14	0.004 26	0.004 25	0.004 23	0.004 19	0.004 16	0.004 13	0.004 08	0.004 07	0.004 01	0.003 90	0.003 74	0.003 55	0.003 11	0.002 65	0.001 84
-10	0.009 16	0.009 18	0.009 07	0.008 96	0.008 87	0.008 78	0.008 73	0.008 59	0.008 42	0.007 95	0.007 35	0.006 72	0.005 45	0.004 33	0.002 68
-8	0.014 63	0.014 88	0.014 65	0.014 44	0.014 29	0.014 19	0.013 98	0.013 65	0.013 20	0.012 09	0.010 82	0.009 55	0.007 27	0.005 47	0.003 15
-6	0.026 8	0.027 2	0.026 7	0.026 3	0.026 2	0.025 8	0.025 0	0.023 8	0.022 4	0.019 37	0.016 42	0.013 75	0.009 62	0.006 81	0.003 63
-5	0.039 4	0.040 0	0.038 9	0.038 4	0.038 3	0.037 2	0.035 4	0.033 0	0.030 3	0.025 0	0.020 3	0.016 46	0.010 94	0.007 49	0.003 86
-4	0.064 0	0.064 0	0.061 7	0.061 2	0.060 5	0.057 4	0.052 7	0.047 4	0.042 1	0.032 5	0.025 1	0.019 54	0.012 30	0.008 16	0.004 06
-3	0.116 7	0.116 5	0.112 8	0.111 4	0.107 9	0.096 5	0.083 2	0.070 5	0.059 3	0.042 1	0.030 5	0.022 8	0.013 58	0.008 75	0.004 22
-2.5	0.177 5	0.172 1	0.167 1	0.162 2	0.153 4	0.130 1	0.106 6	0.086 5	0.070 2	0.047 4	0.033 3	0.024 3	0.014 15	0.009 00	0.004 29
-2	0.295	0.282	0.272	0.255	0.230	0.179 4	0.137 3	0.105 7	0.082 5	0.052 9	0.036 0	0.025 7	0.014 66	0.009 22	0.004 35
-1.5	0.606	0.561	0.514	0.440	0.366	0.250	0.175	0.127 0	0.095 2	0.058 0	0.038 4	0.027 0	0.015 08	0.009 39	0.004 39
-1	...	1.777	1.190	0.816	0.587	0.338	0.216	0.147 7	0.106 6	0.062 1	0.040 2	0.027 9	0.015 38	0.009 52	0.004 43
-0.75	...	4.07	1.821	1.079	0.718	0.382	0.234	0.156 4	0.111 2	0.063 8	0.040 9	0.028 3	0.015 51	0.009 58	0.004 44
-0.5	...	6.45	2.44	1.326	0.838	0.419	0.249	0.163 1	0.114 7	0.065 0	0.041 5	0.028 5	0.015 58	0.009 61	0.004 45
-0.25	...	7.30	2.81	1.492	0.919	0.444	0.258	0.167 5	0.116 9	0.065 8	0.041 8	0.028 7	0.015 64	0.009 62	0.004 46
0	...	7.50	2.92	1.549	0.948	0.453	0.261	0.169 0	0.117 7	0.065 9	0.041 8	0.028 7	0.015 64	0.009 63	0.004 45
0.25	...	7.30	2.81	1.492	0.919	0.444	0.258	0.167 4	0.116 9	0.065 7	0.041 7	0.028 6	0.015 62	0.009 62	0.004 45
0.5	...	6.45	2.44	1.326	0.838	0.419	0.248	0.163 1	0.114 7	0.065 0	0.041 4	0.028 5	0.015 57	0.009 60	0.004 45
0.75	...	4.07	1.821	1.079	0.718	0.382	0.234	0.156 4	0.111 2	0.063 8	0.040 9	0.028 3	0.015 49	0.009 57	0.004 44
1	...	1.779	1.190	0.816	0.587	0.338	0.216	0.147 7	0.106 6	0.062 1	0.040 2	0.027 9	0.015 39	0.009 53	0.004 43
1.5	0.580	0.557	0.515	0.440	0.365	0.250	0.175 0	0.127 0	0.095 2	0.058 0	0.038 4	0.026 9	0.015 08	0.009 39	0.004 40
2	0.283	0.278	0.271	0.255	0.230	0.179 5	0.137 3	0.105 6	0.082 5	0.052 8	0.036 0	0.025 7	0.014 66	0.009 22	0.004 35
2.5	0.169 0	0.169 2	0.166 1	0.162 0	0.153 4	0.130 1	0.106 6	0.086 48	0.070 3	0.047 4	0.033 3	0.024 3	0.014 17	0.009 00	0.004 29
3	0.115 5	0.114 4	0.112 0	0.111 0	0.107 8	0.096 5	0.083 3	0.070 47	0.059 3	0.042 1	0.030 5	0.022 7	0.013 56	0.008 75	0.004 22
4	0.061 8	0.062 5	0.061 0	0.060 9	0.060 3	0.057 4	0.052 7	0.047 41	0.042 1	0.032 6	0.025 1	0.019 54	0.012 29	0.008 16	0.004 06
5	0.038 2	0.039 2	0.038 4	0.038 1	0.038 1	0.037 2	0.035 3	0.032 96	0.030 3	0.025 0	0.020 3	0.016 46	0.010 94	0.007 49	0.003 86
6	0.026 8	0.026 9	0.026 3	0.026 1	0.026 0	0.025 7	0.025 0	0.023 82	0.022 4	0.019 38	0.016 41	0.013 75	0.009 62	0.006 81	0.003 63
8	0.014 48	0.014 62	0.014 45	0.014 27	0.014 18	0.014 11	0.013 94	0.013 63	0.013 19	0.012 07	0.010 83	0.009 55	0.007 27	0.005 48	0.003 15
10	0.008 79	0.008 99	0.008 96	0.008 85	0.008 79	0.008 72	0.008 66	0.008 56	0.008 40	0.007 93	0.007 36	0.006 72	0.005 45	0.004 33	0.002 67
14	0.004 17	0.004 18	0.004 14	0.004 14	0.004 11	0.004 08	0.004 06	0.004 04	0.004 01	0.003 90	0.003 73	0.003 54	0.003 11	0.002 65	0.001 84

$F(r, \theta)$  is the 2D anisotropy function. The subscript  $X$  in the geometry and radial dose functions indicates the point (replace  $X$  by  $P$ ) or line (replace  $X$  by  $L$ ) source approximation. A detailed description of the above parameters can be found in the updated AAPM TG-43 U1 protocol.<sup>11</sup>

## II.E. Calculations of primary and scatter dose separation

The primary and scatter dose separation (PSS) formalism published by Russell *et al.*<sup>32</sup> can be used in convolution/superposition methods<sup>33</sup> to calculate dose distributions around brachytherapy sources in heterogeneous media. This PSS formalism has been recently used to characterize dosimetric properties of HDR <sup>192</sup>Ir and <sup>169</sup>Yb sources.<sup>34</sup> PSS dose formalism is based on the separation of energy deposition into primary and scattered dose components in a given phantom material. Therefore, this model is based on the assumption that the main mechanisms for energy loss from the radiation field of photons leaving the source capsule are well described by the primary and scattered exponential portions of the attenuation. Thus, the total dose is considered to be the superposition of the primary and scattered components such that  $D_{\text{total}} = D_{\text{prim}} + D_{\text{scat}}$ . Following this PSS formalism a photon is considered as a primary photon when it leaves the source capsule without taking account if it has previously interacted inside the source, that is, every photon that escapes from the capsule in the outward direction is a primary photon. When this photon makes its first interaction in the phantom material, it is considered as single scatter until it makes another interaction when it will be considered as a multiple-scattered photon. In the present study, the primary, single-scatter and multiple-scatter photon contributions to dose have been scored separately. The energy spectrum of the primary photons as defined above leaving the capsule has been also binned as described by Taylor and Rogers.<sup>34</sup>

## III. RESULTS AND DISCUSSION

### III.A. TLD measurements and Monte Carlo calculations of dose rate distributions in Solid Water™

Dosimetric characteristics of the IPL <sup>137</sup>Cs source have been determined by TLD measurements and Monte Carlo simulation and the uncertainties of the final results with the two dosimetric techniques were obtained following the TG-43 U1 recommendation.<sup>11</sup> Table I shows the error propagation for the TLD measurement and Monte Carlo data used in these investigations. It should be noted that in this table, the values with “\*” sign were not utilized for derivation of the total uncertainties in experimental radial dose function and 2D anisotropy function. The reason for this exclusion was the fact that these parameters are relative quantities and they are independent of the uncertainties of source calibration and energy correction of the TLD response. Therefore, the underlined italic-bold values are those that have been used for error bars of the radial dose function and 2D anisotropy function.

The dose rate constant of the IPL <sup>137</sup>Cs source TLD measured and MC simulated in the experimental Solid Water™ phantom were found to be  $0.930(\pm 7.3\%)$  and  $0.928(\pm 2.6\%)$  cGy h<sup>-1</sup> U<sup>-1</sup>, respectively. The small difference between both values reflects the accuracy of the source and phantom geometries used in Monte Carlo simulation method. Therefore, this Monte Carlo simulation in water (described in Sec. III B) could be used for clinical application of this source.

The radial dose function of the IPL <sup>137</sup>Cs source was measured and calculated in Solid Water™ using the linear source approximation,  $g_L(r)$ . Figure 2 compares the TLD measured and MC calculated radial dose functions of the IPL source model.

The Monte Carlo derived 2D anisotropy function of the IPL source in Solid Water™ for angles ranging from 0° to 90° were obtained by averaging the values from the four quadrants around the source and are shown in Fig. 3. Taking into account the TLD uncertainties, both TLD measurements and Monte Carlo calculation are compatible. The agreement between these two methods validates the proper selection of the source design, dimensions, and composition materials, particularly the thickness of the end caps, in the simulation technique.

### III.B. Monte Carlo calculations of dose rate distributions in liquid water

Dose rate distribution in liquid water of the IPL source was obtained using Monte Carlo techniques as described in Sec. II C. Table II shows the dose rate distribution for the new source model in water in an along-and-away look-up table.

The Monte Carlo simulated dose rate constant of the IPL source in water was found to be  $\Lambda$

TABLE III. Monte Carlo calculated radial dose functions for the IPL source. These data were fitted to a fifth order polynomial with coefficients  $a_0 = 1.00765$ ,  $a_1 = -7.073 \times 10^{-3}$ ,  $a_2 = -5.680 \times 10^{-4}$ ,  $a_3 = -1.376 \times 10^{-5}$ ,  $a_4 = 1.117 \times 10^{-6}$ , and  $a_5 = -1.608 \times 10^{-8}$  between 0.25 and 20 cm.

Distance $r$ (cm)	$g_L(r)$ ( $L=1.48$ cm)
0.25	1.007
0.5	1.003
0.75	1.002
1.0	1.000
1.5	0.996
2	0.991
3	0.981
4	0.970
5	0.957
6	0.943
7	0.928
8	0.912
10	0.876
12	0.836
15	0.772
20	0.657

TABLE IV. The anisotropy function  $F(r, \theta)$  of the IPL source. The origin is at the geometric center of the source (not at the active center) and the origin of the polar angle is at the tip side of the source (a color coded aluminum ring defines the source tip).

$\theta$ (deg)	$r$ (cm)															
	0.25	0.5	0.75	1	1.5	2	3	4	5	6	7	8	10	12	15	20
0	...	...	...	...	0.912	0.903	0.899	0.899	0.898	0.905	0.910	0.904	0.910	0.923	0.920	0.924
1	...	...	...	...	0.916	0.907	0.906	0.906	0.908	0.911	0.915	0.915	0.919	0.927	0.927	0.936
2	...	...	...	...	0.917	0.912	0.910	0.911	0.913	0.914	0.917	0.921	0.922	0.927	0.932	0.942
3	...	...	...	...	0.917	0.914	0.910	0.909	0.911	0.913	0.915	0.918	0.921	0.925	0.932	0.939
4	...	...	...	...	0.918	0.912	0.905	0.904	0.906	0.909	0.911	0.913	0.919	0.925	0.929	0.936
5	...	...	...	...	0.917	0.909	0.901	0.900	0.902	0.904	0.907	0.910	0.916	0.923	0.928	0.936
6	...	...	...	...	0.913	0.903	0.897	0.898	0.900	0.903	0.907	0.910	0.915	0.922	0.929	0.937
8	...	...	...	...	0.904	0.898	0.898	0.900	0.905	0.908	0.910	0.914	0.920	0.925	0.932	0.940
10	...	...	...	...	0.911	0.907	0.907	0.910	0.914	0.918	0.920	0.923	0.928	0.933	0.940	0.945
15	...	...	...	0.968	0.944	0.940	0.937	0.937	0.940	0.941	0.943	0.944	0.948	0.950	0.954	0.957
20	...	...	1.004	0.981	0.966	0.960	0.957	0.958	0.959	0.960	0.961	0.961	0.964	0.965	0.967	0.968
25	...	1.014	1.002	0.988	0.978	0.974	0.971	0.971	0.971	0.971	0.971	0.971	0.972	0.974	0.975	0.976
30	...	1.009	1.000	0.993	0.985	0.983	0.980	0.978	0.979	0.979	0.979	0.979	0.980	0.981	0.981	0.982
40	...	1.003	0.999	0.997	0.993	0.992	0.990	0.990	0.990	0.989	0.989	0.989	0.989	0.990	0.989	0.990
50	...	1.002	0.999	0.998	0.996	0.996	0.995	0.994	0.995	0.994	0.994	0.994	0.994	0.994	0.995	0.994
60	1.005	1.001	0.999	0.999	0.999	0.999	0.998	0.998	0.998	0.998	0.998	0.997	0.997	0.997	0.998	0.997
70	1.002	1.001	1.000	1.000	0.999	1.000	1.000	0.999	0.999	1.000	0.999	0.999	0.999	0.999	0.999	0.999
80	1.000	1.000	0.999	1.000	1.000	1.000	1.000	1.000	1.001	1.000	1.000	1.000	0.999	1.000	1.000	0.999
90	1	1	1	1	1	1	1	1	1	1	1	1	1	1	1	1
100	1.001	1.000	1.000	1.000	0.999	1.000	1.000	1.000	1.000	1.000	1.000	1.000	0.999	0.999	1.000	1.000
110	1.002	1.001	1.000	1.000	0.999	1.000	0.999	0.999	1.000	0.999	0.999	0.999	0.999	0.999	0.999	0.999
120	1.004	1.001	1.000	0.999	0.998	0.999	0.997	0.997	0.998	0.997	0.997	0.997	0.997	0.998	0.998	0.997
130	...	1.001	0.999	0.998	0.997	0.996	0.996	0.994	0.995	0.994	0.994	0.994	0.994	0.995	0.994	0.994
140	...	1.004	0.999	0.997	0.992	0.992	0.990	0.989	0.990	0.989	0.990	0.989	0.989	0.990	0.990	0.990
150	...	1.009	1.001	0.993	0.985	0.983	0.980	0.979	0.980	0.980	0.980	0.980	0.980	0.981	0.982	0.983
155	...	1.014	1.001	0.988	0.977	0.974	0.971	0.971	0.971	0.972	0.972	0.972	0.973	0.975	0.976	0.977
160	...	...	1.004	0.981	0.964	0.960	0.958	0.958	0.960	0.961	0.961	0.962	0.964	0.965	0.967	0.970
165	...	...	...	0.967	0.945	0.941	0.939	0.940	0.942	0.944	0.946	0.947	0.950	0.953	0.956	0.960
170	...	...	...	...	0.917	0.915	0.915	0.916	0.920	0.922	0.926	0.927	0.932	0.937	0.943	0.947
172	...	...	...	...	0.914	0.909	0.908	0.910	0.913	0.916	0.919	0.922	0.927	0.931	0.939	0.945
174	...	...	...	...	0.928	0.918	0.911	0.910	0.912	0.915	0.918	0.920	0.925	0.930	0.936	0.941
175	...	...	...	...	0.936	0.927	0.918	0.917	0.917	0.918	0.920	0.922	0.927	0.931	0.936	0.942
176	...	...	...	...	0.942	0.934	0.925	0.923	0.924	0.925	0.926	0.927	0.933	0.935	0.939	0.947
177	...	...	...	...	0.943	0.939	0.934	0.931	0.931	0.930	0.931	0.933	0.936	0.938	0.942	0.949
178	...	...	...	...	0.943	0.939	0.937	0.935	0.935	0.935	0.935	0.938	0.939	0.941	0.944	0.948
179	...	...	...	...	0.940	0.935	0.931	0.932	0.934	0.934	0.933	0.936	0.939	0.939	0.943	0.951
180	...	...	...	...	0.932	0.929	0.922	0.925	0.929	0.927	0.928	0.930	0.937	0.930	0.939	0.959

=0.948(±2.6%) cGy h<sup>-1</sup> U<sup>-1</sup>. In addition, the simulated radial dose function (calculated for L=1.48 cm) of this source in water is presented in Table III. Moreover, a fifth order polynomial fit to these data has been introduced for their clinical applications in the treatment planning systems. The coefficients of this polynomial fit are presented in Table III. The Monte Carlo simulated 2D anisotropy function of the source model in liquid water is shown in Table IV at radial distances of distances ranging from 0.25 to 20 cm.

**III.C. Primary and scatter dose separation data**

Primary and scatter dose rate data are tabulated at 12 radial distances ranging from 0.25 to 20 cm and from 0° to 180° polar angles with minimum resolutions of 1°, 2°, 5°, and 10° depending on the angle interval.<sup>35</sup> Figure 4 indicates

the separation of the primary, single, and multiple scattered and the total dose portion of the IPL <sup>137</sup>Cs source in liquid water. In addition, the energy-weighted photon spectrum for this source model is shown in Figure 5.<sup>35</sup>

**IV. CONCLUSIONS**

Dosimetric characteristics of the IPL <sup>137</sup>Cs source (model 67-6520) have been obtained following the AAPM TG-43 U1 formalism using TLD and Monte Carlo methods. The agreement between the measured and Monte Carlo calculated values indicated the proper selection of design, dimensions, and composition material of both the source and the phantom in the Monte Carlo simulations. Using the validated Monte Carlo simulation technique, the clinically recommended TG-43 U1 parameters for this source model have

been determined in liquid water. In addition, a tabulated dose rate distribution in an along-and-away format is provided for benchmark of a treatment planning system or utilization in a quick hand calculation purpose. Moreover, the dose distributions around this source have been parametrized with the PSS formalism. The primary and scattered dose rate tables as well as the energy-weighted photon spectrum are provided for treatment planning systems based on convolution/superposition methods.

## ACKNOWLEDGMENTS

One of the authors (A.S.M.) would like to thank Rebecca F. Duncan, Venkata Rachabathhula, and Curtis Baker for their valuable contributions during the TLD dosimetry procedures. This study was supported in part by Radiation Products and Design, Inc. and by the Generalitat Valencia (Project No. Prometeo/2008/114) and the Spanish Ministerio de Ciencia y Tecnología (Project Nos. FPA2007–65013-C02-01 and FPA2006-12120-C03-02).

- <sup>a)</sup> Author to whom correspondence should be addressed. Electronic mail: alimeig@gmail.com; Telephone: (516)562-2491; Fax: (516)562-1592.
- <sup>1</sup>C. A. Pérez and L. W. Brady, *Principles and Practice of Radiation Oncology*, 3rd ed. (Lippincott Williams and Wilkins, Philadelphia, 1998).
  - <sup>2</sup>D. R. Shearer, *Recent Advances in Brachytherapy Physics* (American Institute of Physics, New York, 1981).
  - <sup>3</sup>P. W. Grigsby, J. F. Williamson, and C. A. Pérez, "Source configuration and dose rates for the Selectron afterloading equipment for gynecologic applicators," *Int. J. Radiat. Oncol., Biol., Phys.* **24**, 321–327 (1992).
  - <sup>4</sup>*The GEC ESTRO Handbook of Brachytherapy*, edited by A. Gerboulet, R. Poetter, J.-J. Mazeron, H. Meertens, and E. Van Limbergen (ESTRO, Leuven, 2002).
  - <sup>5</sup>L. L. Meisberger, R. J. Keller, and R. J. Shalek, "The effective attenuation in water of the gamma rays of gold-198, Ir-192, Cs-137, Ra-226, and Co-60," *Radiology* **90**, 953–957 (1968).
  - <sup>6</sup>V. Krishnaswamy, "Dose distributions about Cs-137 sources in tissue," *Radiology* **105**, 181–184 (1972).
  - <sup>7</sup>J. F. Williamson, "Monte Carlo and analytic calculation of absorbed dose near Cs-137 intracavitary sources," *Int. J. Radiat. Oncol., Biol., Phys.* **15**, 227–237 (1988).
  - <sup>8</sup>R. Waggener, J. Lange, J. Feldmeier, P. Eagan, and S. Martin, "Cs-137 dosimetry table for asymmetric source," *Med. Phys.* **16**, 305–308 (1989).
  - <sup>9</sup>J. F. Williamson, "Monte Carlo based dose rate tables for the Amersham CDCS-J and 3M Model 6500 Cs-137 tubes," *Int. J. Radiat. Oncol., Biol., Phys.* **41**, 959–970 (1998).
  - <sup>10</sup>R. Nath, L. L. Anderson, G. Luxton, K. A. Weaver, J. F. Williamson, and A. S. Meigooni, "Dosimetry of interstitial brachytherapy sources: Recommendations of the AAPM Radiation Therapy Committee Task Group No.43," *Med. Phys.* **22**, 209–234 (1995).
  - <sup>11</sup>M. J. Rivard, B. M. Coursey, L. A. DeWerd, W. F. Hanson, M. Saiful Huq, G. S. Ibbott, M. G. Mitch, R. Nath, and J. F. Williamson, "Update of AAPM Task Group No. 43 Report: A revised AAPM protocol for brachytherapy dose calculations," *Med. Phys.* **31**, 663–674 (2004).
  - <sup>12</sup>E. Casal, F. Ballester, J. L. Lluch, J. Perez-Calatayud, and F. Lliso, "Monte Carlo calculations of dose rate distribution around the Amersham CDCS-M-type Cs-137 source," *Med. Phys.* **27**, 132–140 (2000).
  - <sup>13</sup>F. Ballester, J. L. Lluch, Y. Limami, M. A. Serrano, E. Casal, J. Pérez-Calatayud, and F. Lliso, "A Monte-Carlo investigation of the dosimetric characteristics of the CSM11 <sup>137</sup>Cs source from CIS," *Med. Phys.* **27**, 2182–2189 (2000).
  - <sup>14</sup>J. Pérez-Calatayud, F. Lliso, F. Ballester, M. A. Serrano, J. L. Lluch, Y. Limami, V. Puchades, and E. Casal, "A Monte-Carlo study of dose rate distributions around the specially asymmetric CSM3-a Cs-137 source," *Phys. Med. Biol.* **46**, N169–N173 (2001).
  - <sup>15</sup>J. Pérez-Calatayud, D. Granero, E. Casal, F. Ballester, and V. Puchades,

- "Monte Carlo and experimental derivation of TG-43 dosimetric parameters for CSM-type Cs-137 sources," *Med. Phys.* **32**, 28–36 (2005).
- <sup>16</sup>J. Pérez-Calatayud, F. Ballester, J. L. Lluch, M. A. Serrano-Andrés, E. Casal, V. Puchades, and Y. Limami, "Monte Carlo calculation of dose rate distributions around the Walstam CDC-K-type <sup>137</sup>Cs sources," *Phys. Med. Biol.* **46**, 2029–2040 (2001).
  - <sup>17</sup>J. Pérez-Calatayud, F. Ballester, M. A. Serrano-Andrés, J. L. Lluch, V. Puchades, Y. Limami, and E. Casal, "Dosimetric characteristics of the CDC-type miniature cylindrical <sup>137</sup>Cs brachytherapy sources," *Med. Phys.* **29**, 538–543 (2002).
  - <sup>18</sup>J. Pérez-Calatayud, D. Granero, F. Ballester, V. Puchades, and E. Casal, "Monte Carlo dosimetric characterization of the Cs-137 selectron/LDR source: Evaluation of applicator attenuation and superposition approximation effects," *Med. Phys.* **31**, 493–499 (2004).
  - <sup>19</sup>L. Liu, S. C. Prasad, and D. A. Bassano, "Determination of Cs-137 dosimetry parameters according to the AAPM TG-43 formalism," *Med. Phys.* **31**, 477–483 (2004).
  - <sup>20</sup>J. Pérez-Calatayud, D. Granero, F. Ballester, E. Casal, R. Cases, and S. Agramunt, "Technical note: Monte Carlo derivation of TG-43 dosimetric parameters for radiation therapy resources and 3M Cs-137 sources," *Med. Phys.* **32**, 2464–2470 (2005).
  - <sup>21</sup>S. Meigooni, D. M. Gearheart, and K. Sowards, "Experimental determination of dosimetric characteristics of Best<sup>®</sup> <sup>125</sup>I brachytherapy source," *Med. Phys.* **27**, 2168–2173 (2000).
  - <sup>22</sup>A. S. Meigooni, Z. Bharucha, M. Yoe-Sein, and K. Sowards, "Dosimetric characteristics of the Best<sup>®</sup> double-wall <sup>103</sup>Pd brachytherapy source," *Med. Phys.* **28**, 2568–2575 (2001).
  - <sup>23</sup>A. S. Meigooni, H. Panth, V. Mishra, and J. F. Williamson, "Instrumentation and dosimeter-size artifacts in quantitative thermoluminescence dosimetry of low-dose fields," *Med. Phys.* **22**, 555–561 (1995).
  - <sup>24</sup>S. Agostinelli *et al.*, "Geant4—a simulation toolkit," *Nucl. Instrum. Methods Phys. Res. A* **506**, 250–303 (2003); see also <http://geant4.web.cern.ch/geant4/>.
  - <sup>25</sup>Z. Li, R. K. Das, L. A. DeWerd, G. S. Ibbott, A. S. Meigooni, J. Perez-Calatayud, M. J. Rivard, R. S. Sloboda, and J. F. Williamson, "Dosimetric prerequisites for routine clinical use of photon emitting brachytherapy sources with average energy higher than 50 keV," *Med. Phys.* **34**, 37–40 (2007).
  - <sup>26</sup>J. Perez-Calatayud, D. Granero, M. Rivard, C. Melhus, M. Pujades, and F. Ballester, "Evaluation of electronic equilibrium conditions near brachytherapy sources," *Med. Phys.* **35**, 2971 (2008).
  - <sup>27</sup>D. Cullen, J. H. Hubbell and L. Kissel, "EPDL97: The evaluated photon data library, '97 version," Lawrence Livermore National Laboratory Report No. UCRL-LR-50400, 6, Rev. 5 (1997).
  - <sup>28</sup>J. F. Williamson, "Monte Carlo evaluation of kerma at a point for photon transport problems," *Med. Phys.* **14**, 567–576 (1987).
  - <sup>29</sup>A. S. Meigooni, S. B. Awan, N. S. Thompson, and S. A. Dini, "Updated Solid Water<sup>TM</sup> to water conversion factors for <sup>125</sup>I and <sup>103</sup>Pd brachytherapy sources," *Med. Phys.* **33**, 3988–3992 (2006).
  - <sup>30</sup>C. S. Melhus and M. J. Rivard, "Approaches to calculating AAPM TG-43 brachytherapy dosimetry parameters for <sup>137</sup>Cs, <sup>125</sup>I, <sup>192</sup>Ir, <sup>103</sup>Pd, and <sup>169</sup>Yb sources," *Med. Phys.* **33**, 1729–1737 (2006).
  - <sup>31</sup>J. Pérez-Calatayud, D. Granero, and F. Ballester, "Phantom size in brachytherapy source dosimetric studies," *Med. Phys.* **31**, 2075–2081 (2004).
  - <sup>32</sup>K. R. Russell, A. K. Carlsson-Tedgren, and A. Ahnesjö, "Brachytherapy source characterization for improved dose calculations using primary and scatter dose separation," *Med. Phys.* **32**, 2739–2752 (2005).
  - <sup>33</sup>J. F. Williamson, R. S. Baker, and Z. Li, "A convolution algorithm for brachytherapy dose computation in heterogeneous geometries," *Med. Phys.* **18**, 1256–1265 (1991).
  - <sup>34</sup>R. E. P. Taylor and D. W. O. Rogers, "EGSnrc Monte Carlo calculated dosimetry parameters for <sup>192</sup>Ir and <sup>169</sup>Yb brachytherapy sources," *Med. Phys.* **35**, 4933–4944 (2008).
  - <sup>35</sup>See EPAPS Document No. E-MPHYA6-36-054910 for the numerical values of the parameters and functions of TG-43 U1 formalism for the IPL in EXCEL spreadsheet format. The primary and scatter photon dose contributions as well as the energy-weighted photon spectrum are also provided. For more information on EPAPS, see <http://www.aip.org/pubservs/epaps.html>.